ORIGINAL ARTICLE

The expression and mechanism of Sirt1 and AMPK in non-small cell lung cancer

Fushen Yang

Department of Thoracic Surgery, Affiliated Hospital of Hebei Engineering University, Handan, China

Summary

Purpose: To investigate the expression of sirtuin type 1 (Sirt1) and adenosine 5'-monophosphate (AMP)-activated protein kinase (AMPK) in non-small cell lung cancer (NSCLC), and to explore the mechanism of their functions in NSCLC.

Methods: Cancer tissues (NSCLC group) and the adjacent normal healthy tissues (control group) of 50 patients with NSCLC were selected, and H&E staining was performed to identify the histopathological differences. Reverse transcription polymerase chain reaction (RT-PCR), immunofluorescence staining and Western blot were performed to detect the expression of Sirt1 and AMPK in tissues of NSCLC group and control group. SPSS17.0 statistical software was used to analyze the differences in the expression of Sirt1 and AMPK between control group and NSCLC group.

Results: Significant differences in histopathological structure were found between NSCLC and control group by H&E

staining. Compared with control group, cell structure in NSCLC group was destroyed and condensed nuclei were observed, indicating the lung injury. Results of RT-PCR, immunofluorescence staining and Western blot showed that the expression levels of Sirt1 and AMPK were significantly lower in the NSCLC group than in the control group at both mRNA and protein levels. Results of variance analysis showed significant differences in the expression levels of Sirt1 and AMPK between control group and NSCLC group ($p<0.01$).

Conclusion: The abnormal expression of Sirt1 and AMPK was closely related to the occurrence and development of NSCLC.

Key words: adenosine 5'-monophosphate (AMP) -activated protein kinase (AMPK), non-small cell lung cancer, sirtuin type 1 (Sirt1)

Introduction

With economic development and increased effects of environmental and other factors, lung cancer has become a common malignant tumor that seriously affects people's health [1-3]. Pathogenesis of NSCLC is very complex [4]. Sirt1 and AMPK have recently been reported to be closely correlated with the development of NSCLC [5,6]. In this study, H&E staining was performed to detect the histopathological differences between the control group and the NSCLC group. In addition, expression levels of Sirt1 and AMPK in both NSCLC and control groups were detected by RT-PCR, immunofluorescence and Western blot to investigate the differences in the expression of Sirt1 and AMPK between NSCLC and control groups, so as to explore the roles of Sirt1 and AMPK in the development of NSCLC and provide new insights to the genetic diagnosis and treatment of NSCLC.

Methods

General information

Cancer tissue and adjacent healthy tissue specimens were obtained from 50 patients with NSCLC who were treated in our hospital from 2014 to 2016. All patients signed informed consent. Patients included 32 males and 18 females, and the ages ranged from 45 to 72 years. Tissues were fixed in 10% formalin and embedded in paraffin, followed by H&E staining and immunofluorescence staining. The remaining tissues were used for RT-PCR and Western blot.

Major reagents

Trizol total RNA extraction kit and reverse transcription kit (TIANGEN, Bejing, China); BCA protein quantitative kit and IP lysate (Beyotime Biotechnology, Shanghai, China); total protein extraction kit (KeyGEN BioTECH, Jiangsu, China); anti-GAPDH, anti-Sirt1 and anti-AMPK monoclonal antibodies, secondary antibody and immunofluorescence secondary antibody (CST, Boston, USA). All reagents were purchased.

Histopathological examination

Tissues of control group and NSCLC group were embedded in paraffin and cut into 5 mm sections. Routine method was used to perform H&E staining. The stained tissues were observed under an optical microscope (x200, Nikon Eclipse TE2000-U, Nikon, Japan) for histopathological study.

Real-time PCR

Tissue in the control and NSCLC groups were mixed in Trizol reagent to make homogenate. The homogenate was kept at room temperature for 5 min for complete lysis, followed by centrifugation (12000 g, 4°C) for 5 min to collect the supernatant. The supernatant was mixed with chloroform and kept at room temperature for 5 min, followed by centrifugation (12000 g, 4°C) for 15 min to collect the supernatant. The supernatant mixed with the same volume of isopropanol was kept at room temperature for 10 min, followed by centrifugation (12000 g, 4°C) for 10 min to collect the precipitate. After washing with 75% ethanol, the precipitate was dissolved in RNase-free water. The optical density (OD) 260 /OD280 ratio was determined and the RNA concentration was measured. Primers (Sangon, Shanghai, China) used for PCR reactions are listed in Table 1.

Immunofluorescence analysis

Paraffin-embedded tissue sections were subjected to dewaxing by xylene and hydration by passing a series of graded concentrations of ethanol, followed by antigen retrieval and washing with 0.01 M PBS (pH 7.4) for 3 times, 5 min each time. After blocking in 10% BSA at 37°C, diluted fluorescence labeled antibody (1:70) was added, followed by incubation in wet box overnight at 4°C. After washing with 0.01 M PBS (pH 7.4) for 3 times, 5 min each time, fluorescence labeled secondary antibody (1:100) was added and incubated at 37°C for 2 hrs in wet box. Finally, slides were sealed with buffered glycerol and observed under an upright fluorescence microscope.

Western blot

Tissues of the control group and NSCLC group were washed with pre-cooled saline, and total protein was extracted using a total protein extraction kit. Tissues were ground in immunologic precipitation lysate containing phenylmethanesulfone fluoride (PMSF) and protease inhibitors, followed by centrifugation (4°C, 12000 g) for 10 min to collect the supernatant. The supernatant was further centrifuged (4°C, 12000 g) for 20 min to collect the supernatant again. Protein concentration was measured using BCA protein quantification kit, and 10 μl of protein from the sample was subjected to SDS-PAGE electrophoresis under 220V until bromophenol blue reached the bottom of the gel. Protein was then transferred to polyvinylidene fluoride (PVDF) membrane, followed by blocking with 5% skimmed milk at room temperature for 3 hrs on a shaker. After that, membranes were incubated with the corresponding primary antibodies (1:1000) overnight at 4°C. After washing with tris-buffered saline and tween 20 (TBST) for 3 times, 10 min each time, membranes were incubated with secondary antibody (1:2000) at room temperature for 1 hr. After washing with TBST for 3 times, 10 min each time, electrochemiluminescence (ECL) solution was added for color development.

Statistics

Experimental data were expressed as mean ± SD and were processed by SPSS 17.0 statistical software. The means between groups were compared using the t-test, while the means among groups were compared using one-way ANOVA. $P<0.05$ was considered as statistically significant.

Table 1. Sequences of primers used in real-time PCR

Gene	Forward primer (5'-3')	Reverse primer (5'-3')
Sirt1	TTCAGGTCAAGGGATGGTATTT	TGTTCCAGCGTGTCTATGTTCT
AMPK	CGCCAGGGTTTTCCCAGTCACGAC	GAGCGGATAACAATTTACAGG
β-actin	CTGGGACGACATGGAGAAAA	AAGGAAGGCTGGAAGAGTGC

Results

Observation of pathological changes by H&E staining

Tissue sections of control and NSCLC groups were stained with H&E to observe histopathological changes. Compared with the control group, cell structure was destroyed and nuclei were seriously condensed in the NSCLC group, indicating severe lung injury (cancerization) (Figure 1).

Expression of Sirt1 and AMPK detected by RT-PCR

As shown in Figure 2, the expression levels of Sirt1 and AMPK were significantly lower in the NSCLC group than in the control group (p<0.01).

Expression of Sirt1 in the control and NSCLC group detected by immunofluorescence staining

As shown in Figure 3, the results of immunofluorescence staining showed that Sirt1 was highly expressed in the control group, but the expression level in NSCLC was relatively low. These results suggest that the expression level of Sirt1 was higher in the control group than in the NSCLC group.

Expression of AMPK in the control and NSCLC group detected by immunofluorescence staining

As shown in Figure 4, immunofluorescence staining showed that AMPK was highly expressed in the control group but rarely in the NSCLC
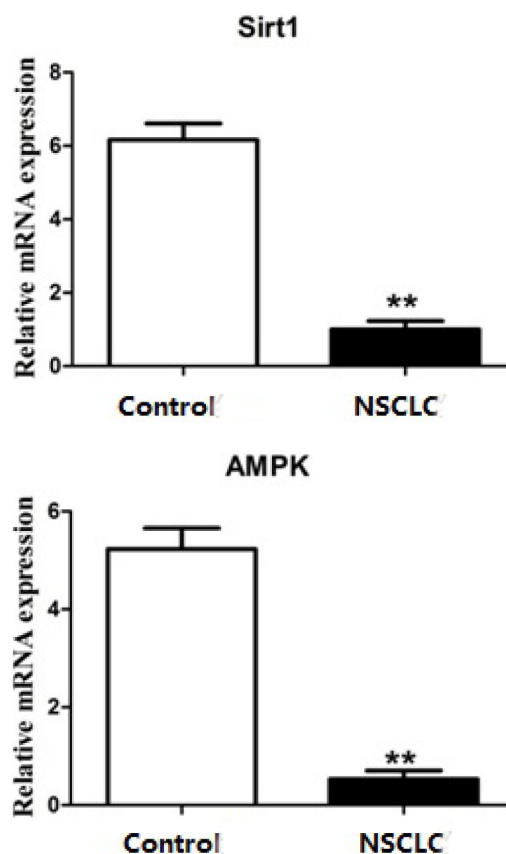

Figure 2. Expression of Sirt1 and AMPK in NSCLC and control groups. The expression levels of Sirt1 and AMPK mRNA in the NSCLC group were significantly lower than those in the control group. **compared with the control group, p<0.01. All experiments were performed in triplicate.
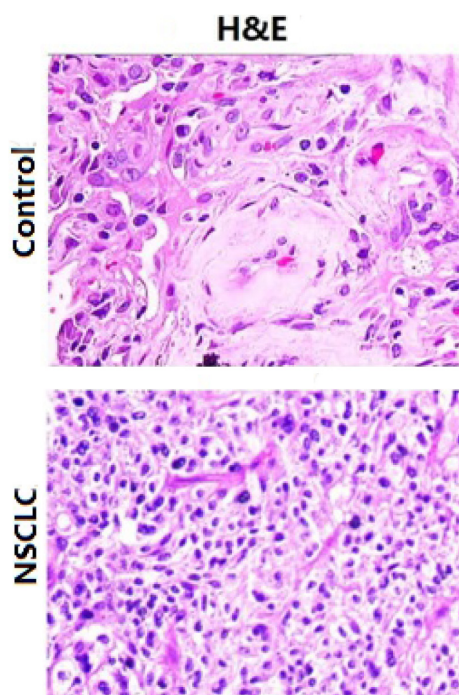

Figure 1. H&E staining results of tissues in the control and NSCLC group (×200). Compared with the control group, cell structure in the NSCLC group was destroyed and nuclei were condensed (cancerization).
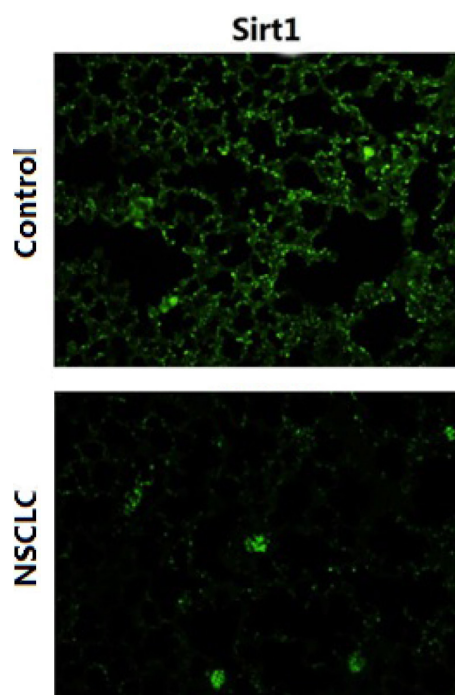

Figure 3. Immunofluorescence staining results of Sirt1 in the control and the NSCLC group (×400). Sirt1 was highly expressed in the control group and rarely expressed in the NSCLC group.

group. These results suggest that the expression level of Sirt1 was higher in the control group compared with the NSCLC group.

Expression of Sirt1 and AMPK in the control and NSCLC group detected by Western blot

As shown in Figure 5, protein was extracted from the tissue of the control group and NSCLC group for Western blot. The results showed that the expression levels of Sirt1 and AMPK were significantly lower in the NSCLC group than in the control group (p<0.01).
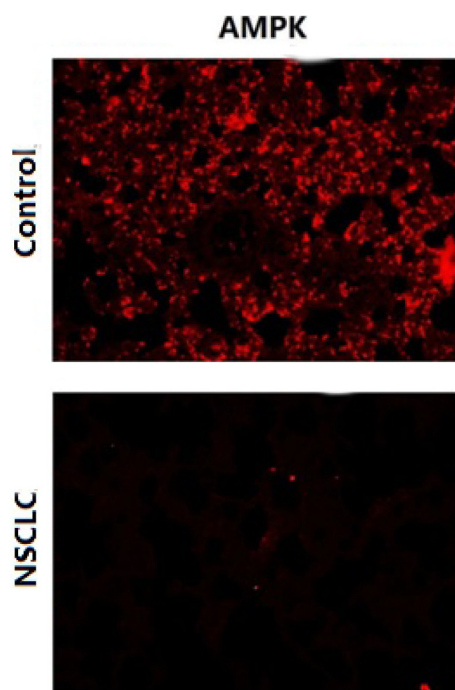

Figure 4. Immunofluorescence staining results of AMPK in the control and the NSCLC group (×400). AMPK was highly expressed in the control group but the expression level was relatively low in the NSCLC group.

Figure 5. Expression of Sirt1 and AMPK proteins in the control and the NSCLC group. Expression levels of Sirt1 and AMPK in the NSCLC group were significantly lower in the NSCLC group than in the control group. **compared with control group, p<0.01. All experiments were performed in triplicate.

Discussion

In recent years, numerous studies have shown that the incidence of lung cancer is gradually increasing, seriously affecting people's health and life [7-9]. NSCLC is a common type of lung cancer with high incidence [10]. Therefore, the development of safe and effective methods for the treatment of NSCLC is an ever-lasting target. The development of NSCLC is closely related to the expression of a variety of genes. The development of treatment using these genes as targets may improve treatment outcomes of this disease.

As a nicotinamide adenine dinucleotide–dependent deacetylase in mammals, Sirt1 can participate in the regulation of transcription of related genes and the activities of metabolic enzymes by regulatin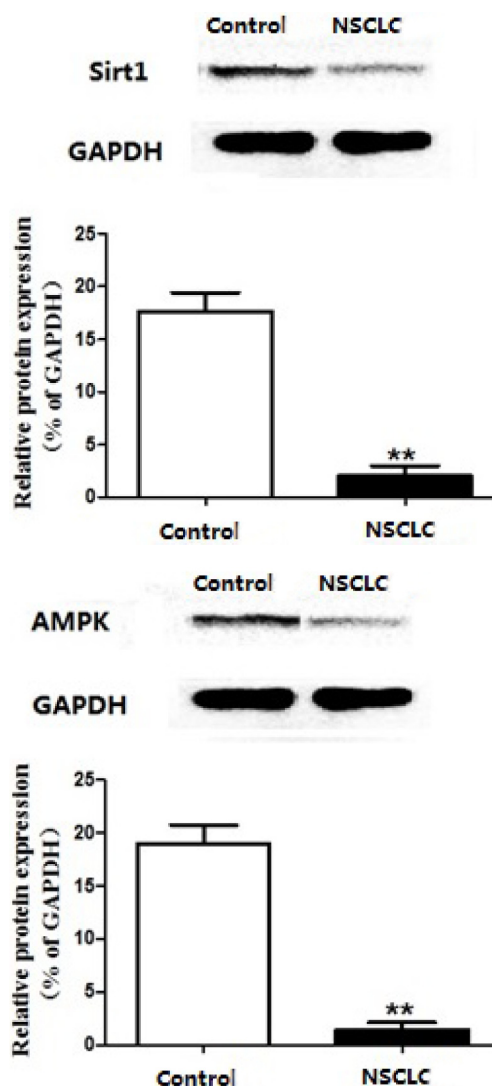g the acetylation of histones, related transcription factors and signal transduction molecules [11-13]. As a multi-functional protein deacetylase, Sirt1 has attracted significant attention due to its roles in extending life span, regulating cell cycle and apoptosis, regulating metabolism and many other physiological cellular processes [14,15]. Studies have shown that Sirt1 played an important role in the treatment of diabetes mellitus, obesity and other diseases through its roles in cell survival and apoptosis, and lipid metabolism [16]. AMPK is widely in the organism and plays a key role in cell energy metabolism and cell growth differentiation. As an extremely important protein kinase, the biological effects of AMPK in the clinical treatment of various diseases have been well studied [17,18]. It is generally accepted that AMPK has great potentials in the treatment

of cardiovascular disease, diabetes, obesity, central nervous diseases and cancer [19,20].

In this study, NSCLC tissue and normal healthy tissue were stained with H&E to observe the histopathological differences between them. RT-PCR, immunofluorescence staining and Western blot were performed to assess the expression of Sirt1 and AMPK at both mRNA and protein levels. The results of this study showed that Sirt1 and AMPK were expressed in tissues of the control group and rarely in the tissues of NSCLC

group. Significant differences in the expression levels of Sirt1 and AMPK were found between the control and NSCLC group by RT-PCR and Western blot (p<0.05). These data suggested that Sirt1 and AMPK genes were involved in the development of NSCLC. These two genes may potentially be targets for the treatment of NSCLC.

Conflict of interests

The authors declare no conflict of interests.

References

1. Cappuzzo F, Gregorc V, Rossi E et al. Gefitinib in pretreated non-small-cell lung cancer (NSCLC): Analysis of efficacy and correlation with HER2 and epidermal growth factor receptor expression in locally advanced or metastatic NSCLC. J Clin Oncol 2003;21:2658-63.

2. Ando M, Okamoto I, Yamamoto N et al. Predictive factors for interstitial lung disease, antitumor response, and survival in non-small-cell lung cancer patients treated with gefitinib. J Clin Oncol 2006;24:2549-56.

3. Zhao Z, Su Z, Zhang W, Luo M, Wang H, Huang L. A randomized study comparing the effectiveness of microwave ablation radioimmunotherapy and postoperative adjuvant chemoradiation in the treatment of non-small cell lung cancer. JBUON 2016;21:326-32.

4. Cortes-Funes H, Gomez C, Rosell R et al. Epidermal growth factor receptor activating mutations in Spanish gefitinib-treated non-small-cell lung cancer patients. Ann Oncol 2005;16:1081-6.

5. Chua KF, Mostoslavsky R, Lombard DB et al. Mammalian SIRT1 limits replicative life span in response to chronic genotoxic stress. Cell Metab 2005;2:67-76.

6. Zhang YJ, Xiang H, Liu JS, Li D, Fang ZY, Zhang H. Study on the mechanism of AMPK signaling pathway and its effect on apoptosis of human hepatocellular carcinoma SMMC-7721 cells by curcumin. Eur Rev Med Pharmacol Sci 2017;21:1144-50.

7. Bell DW, Lynch TJ, Haserlat SM et al. Epidermal growth factor receptor mutations and gene amplification in non-small-cell lung cancer: Molecular analysis of the IDEAL/INTACT gefitinib trials. J Clin Oncol 2005;23:8081-92.

8. Gatzemeier U, Pluzanska A, Szczesna A et al. Results of a phase III trial of erlotinib (OSI-774) combined with cisplatin and gemcitabine (GC) chemotherapy in advanced non-small cell lung cancer (NSCLC). J Clin Oncol 2004;22:7010.

9. Jiang HL, Jiang LM, Han WD. Wnt/beta-catenin signaling pathway in lung cancer stem cells is a potential target for the development of novel anticancer drugs. JBUON 2015;20:1094-1100.

10. Lynch TJ, Bell DW, Sordella R et al. Activating mutations in the epidermal growth factor receptor underlying responsiveness of non-small-cell lung cancer to gefitinib. N Engl J Med 2004;350:2129-39.

11. Picard F, Kurtev M, Chung N et al. Sirt1 promotes fat mobilization in white adipocytes by repressing PPAR-gamma. Nature 2004;429:771-6.

12. Bordone L, Guarente L. Calorie restriction, SIRT1 and metabolism: Understanding longevity. Nat Rev Mol Cell Biol 2005;6:298-305.

13. Lin N, Li XY, Zhang HM, Yang Z, Su Q. MicroR-NA-199a-5p mediates high glucose-induced reactive oxygen species production and apoptosis in INS-1 pancreatic beta-cells by targeting SIRT1. Eur Rev Med Pharmacol Sci 2017;21:1091-8.

14. Cheng HL, Mostoslavsky R, Saito S et al. Developmental defects and p53 hyperacetylation in Sir2 homolog (SIRT1)-deficient mice. Proc Natl Acad Sci U S A 2003;100:10794-9.

15. Lagouge M, Argmann C, Gerhart-Hines Z et al. Resveratrol improves mitochondrial function and protects against metabolic disease by activating SIRT1 and PGC-1alpha. Cell 2006;127:1109-22.

16. Li X, Zhang S, Blander G, Tse JG, Krieger M, Guarente L. SIRT1 deacetylates and positively regulates the nuclear receptor LXR. Mol Cell 2007;28:91-106.

17. Akman HO, Sampayo JN, Ross FA et al. Fatal infantile cardiac glycogenosis with phosphorylase kinase deficiency and a mutation in the gamma2-subunit of AMP-activated protein kinase. Pediatr Res 2007;62:499-504.

18. Claret M, Smith MA, Batterham RL et al. AMPK is essential for energy homeostasis regulation and glucose sensing by POMC and AgRP neurons. J Clin Invest 2007;117:2325-36.

19. Funai K, Cartee GD. Inhibition of contraction-stimulated AMP-activated protein kinase inhibits contraction-stimulated increases in PAS-TBC1D1 and glucose transport without altering PAS-AS160 in rat skeletal muscle. Diabetes 2009;58:1096-1104.

20. Gaidhu MP, Fediuc S, Anthony NM et al. Prolonged AICAR-induced AMP-kinase activation promotes energy dissipation in white adipocytes: Novel mechanisms integrating HSL and ATGL. J Lipid Res 2009;50:704-15.